PRRL-76-CR-58

ERDA/JPL/954465-76/3
Distribution Category UC-63

SILICON SHEET GROWTH BY THE INVERTED STEPANOV TECHNIQUE

K. M. Kim, G. W. Cullen, S. Berkman,
and A. E. Bell

RCA Laboratories
Princeton, New Jersey 08540

NOTICE
This report was prepared as an account of work sponsored by the United States Government. Neither the United States nor the United States Energy Research and Development Administration, nor any of their employees, nor any of their contractors, subcontractors, or their employees, makes any warranty, express or implied, or assumes any legal liability or responsibility for the accuracy, completeness or usefulness of any information, apparatus, product or process disclosed, or represents that its use would not infringe privately owned rights.

QUARTERLY REPORT NO. 3

December 1976

This work was performed for the Jet Propulsion Laboratory, California Institute of Technology, under NASA Contract NAS7-100 for the U. S. Energy Research and Development Administration, Division of Solar Energy.

The JPL Low-Cost Silicon Solar Array Project is funded by ERDA and forms part of the ERDA Photovoltaic Conversion Program to initiate a major effort toward the development of low-cost solar arrays.

Prepared Under Contract No. 954465 For
JET PROPULSION LABORATORY
CALIFORNIA INSTITUTE OF TECHNOLOGY
Pasadena, California 91103

DISTRIBUTION OF THIS DOCUMENT IS UNLIMITED

DISCLAIMER

This report was prepared as an account of work sponsored by an agency of the United States Government. Neither the United States Government nor any agency thereof, nor any of their employees, makes any warranty, express or implied, or assumes any legal liability or responsibility for the accuracy, completeness, or usefulness of any information, apparatus, product, or process disclosed, or represents that its use would not infringe privately owned rights. Reference herein to any specific commercial product, process, or service by trade name, trademark, manufacturer, or otherwise does not necessarily constitute or imply its endorsement, recommendation, or favoring by the United States Government or any agency thereof. The views and opinions of authors expressed herein do not necessarily state or reflect those of the United States Government or any agency thereof.

DISCLAIMER

Portions of this document may be illegible in electronic image products. Images are produced from the best available original document.

PREFACE

This Quarterly Report No. 3, prepared by RCA Laboratories, Princeton, New Jersey 08540, describes work performed under Contract No. 954465 in the Process and Applied Materials Research Laboratory, P. Rappaport, Director. G. W. Cullen is the Group Head and the Project Supervisor. K. M. Kim is the Project Scientist. Others who participated in the research are S. Berkman, A. E. Bell (thermal analysis), H. E. Temple, and R. E. Novak.

The JPL Project Monitor is K. M. Koliwad.

TABLE OF CONTENTS

Section		Page
I.	SUMMARY	1
II.	INTRODUCTION	2
III.	PROGRESS AND TECHNICAL DISCUSSION	5
	A. IST Silicon Ribbon Growth with SiO_2 Die	5
	1. Ribbon Growth with a Standard V-Shaped Susceptor	7
	2. Ribbon Growth with a Modified V-Shaped Susceptor	10
	B. Solar Cells Fabricated in Silicon Epitaxially Deposited on IST Ribbon	13
	C. Thermal Analysis of the IST Ribbon Growth	14
IV.	CONCLUSIONS AND FUTURE PLANS	22
REFERENCES		23
APPENDIX A - New Technology		25
APPENDIX B - Program Plan		26
APPENDIX C - Manhours and Costs		27

LIST OF ILLUSTRATIONS

Figure		Page
1.	Schematic drawing of silicon ribbon growth by the inverted Stepanov technique (IST)	3
2.	Cross-sectional view of the V-shaped graphite susceptor; (a) a standard type and (b) a modified susceptor to decrease the vertical temperature gradient inside the susceptor	5
3.	Cross-sectional view of the thermal trimmers used to control the thermal gradients at the solid-liquid ribbon growth interface	6
4.	Cross section of fused silica dies of three different designs . .	7
5.	Ribbon growth configuration with the modified susceptor and an L-shaped trimmer	11
6.	Thermal gradients with the modified susceptor; (a) horizontal temperature distribution along the die edge, and (b) vertical temperature gradient at the die edge	12
7.	Photomicrograph of a solar cell fabricated in the epitaxially grown layers on the IST silicon ribbon grown with BN die	14
8.	I-V characteristics of the epitaxial solar cells on the IST silicon ribbon and Czochralski silicon wafer	15
9.	Ribbon temperature profiles for 0.0375 x 1.0 cm ribbon, ribbon clamp 3.0 cm from die. Curve I: 300°K uniform ambient V = 0.10 cm/s. Curve II: 1300°K uniform ambient V = 0.05 cm/s. Curve III: Linear ambient from 1650°K at the die to 300°K at the clamp, V = 0.03 cm/s.	17
10.	Curvature $\left\|\frac{d^2T}{dx^2}\right\|$ of the ribbon temperature profiles shown in Fig. 11	18
11.	Temperature profile along 0.0375-cm-thick ribbon for various ambient conditions and growth rates. In all cases the ribbon is clamped at 800°K at a distance of 0.5 cm from the die aperture. Curve I: V = 0.0, no radiation or convection heat loss. Curve II: Uniform ambient 800°K, V = 0.125 cm/s. Curve III: Linear ambient 1600°K at x = 0, 1300°K at x = 0.5 cm, V = 0.08 cm/s. Curve IV: Linear ambient 1600°K at x = 0, 1400°K at x = 0.5 cm, V = 0.08 cm/s	20

SECTION I

SUMMARY

Efforts were continued to overcome the instabilities experienced when silica dies are used for growth of silicon ribbon in the inverted Stepanov configuration. These instabilities are associated primarily with the formation and evolution of the silicon monoxide; the escape of the gas causes hysteresis of the contact angle and mechanical vibration of the melt. As a result of this, the meniscus during the ribbon growth is not "pinned" at the die edge, but is in constant motion.

The V-shaped susceptor has been modified to decrease the vertical gradient inside the susceptor in order to minimize the SiO formation and the related hysteresis. Furthermore, in an effort to improve "pinning" the meniscus at the die edge, a sharp-edged die was used. A pressure differential has also been applied across the melt in an effort to suppress the hysteresis. Various types of thermal trimmers have been tried to provide suitable thermal gradients at the solid-liquid ribbon growth interface. So far, the instabilities have not been suppressed sufficiently to allow for stable ribbon growth.

The thermal stress exerted on the ribbon during growth can be reduced by minimizing the curvature in the ribbon temperature profile. Our computer model shows that in principle it is possible to achieve a high growth rate simultaneously with a linear ribbon temperature profile by shortening the distance between the die aperture and the ribbon clamp. This results in an increased heat flux (and therefore temperature gradient) at the molten zone boundary due to the increased conduction loss to the clamp. The ribbon temperature profile can then be linearized by tailoring the ambient temperature profile so that the radiative and convective heat transfer between the ribbon and the environment compensate for the temperature dependence in the thermal conductivity of the silicon.

SECTION II

INTRODUCTION

Work on the Stepanov [1] shaped crystal growth process was originally initiated in order to provide more latitude in the choice of die materials for silicon ribbon growth. The dissolution of carbon dies, and the subsequent formation of silicon carbide in the growing ribbon, has been identified as one source of degradation of the crystal structure of the ribbon. The use of a process which does not require that the die be wetted provides some flexibility in the choice of die materials since wetting implies some degree of chemical reaction with the die.

The lack of capillary rise associated with wetting of the die can be at least partially overcome by gravity feed of the source material through the shaping slot. For this reason the conventional Stepanov method was inverted so that the feed flows and the crystal is pulled in a downward direction. For some slot shapes the gravity feed is sufficient. In order to provide further flexibility in control of the material feed, particularly for the growth of thin ribbons, a pressure differential has been applied across the melt. The application of the pressure not only gives latitude in the shape of the slot, but has the additional advantage that it can be altered during the growth of the ribbon. To some extent the natural flow with gravity can be influenced through surface tension forces by attachment of a solid portion of the feed to the liquid. The molten feed can be pushed or pulled by manipulation of the solid which protrudes above the top of the susceptor assembly. It is the usual situation in shaped crystal growth that the conditions required to initiate growth must be altered in order to realize a steady-state crystal growth condition. Independent control of the pressure across the melt and the position of the solid feed provides latitude in executing the needed changes in the supply of the source material.

After initial experiments with a flat-die inverted Stepanov configuration, a V-shaped die was designed and put into use (Fig. 1). The V-shape was originally introduced to compensate for the lack of mechanical strength

---

1. A. V. Stepanov et al., Bull. Acad. Sci. USSR, Phys. Series 33, 1826 (1969).

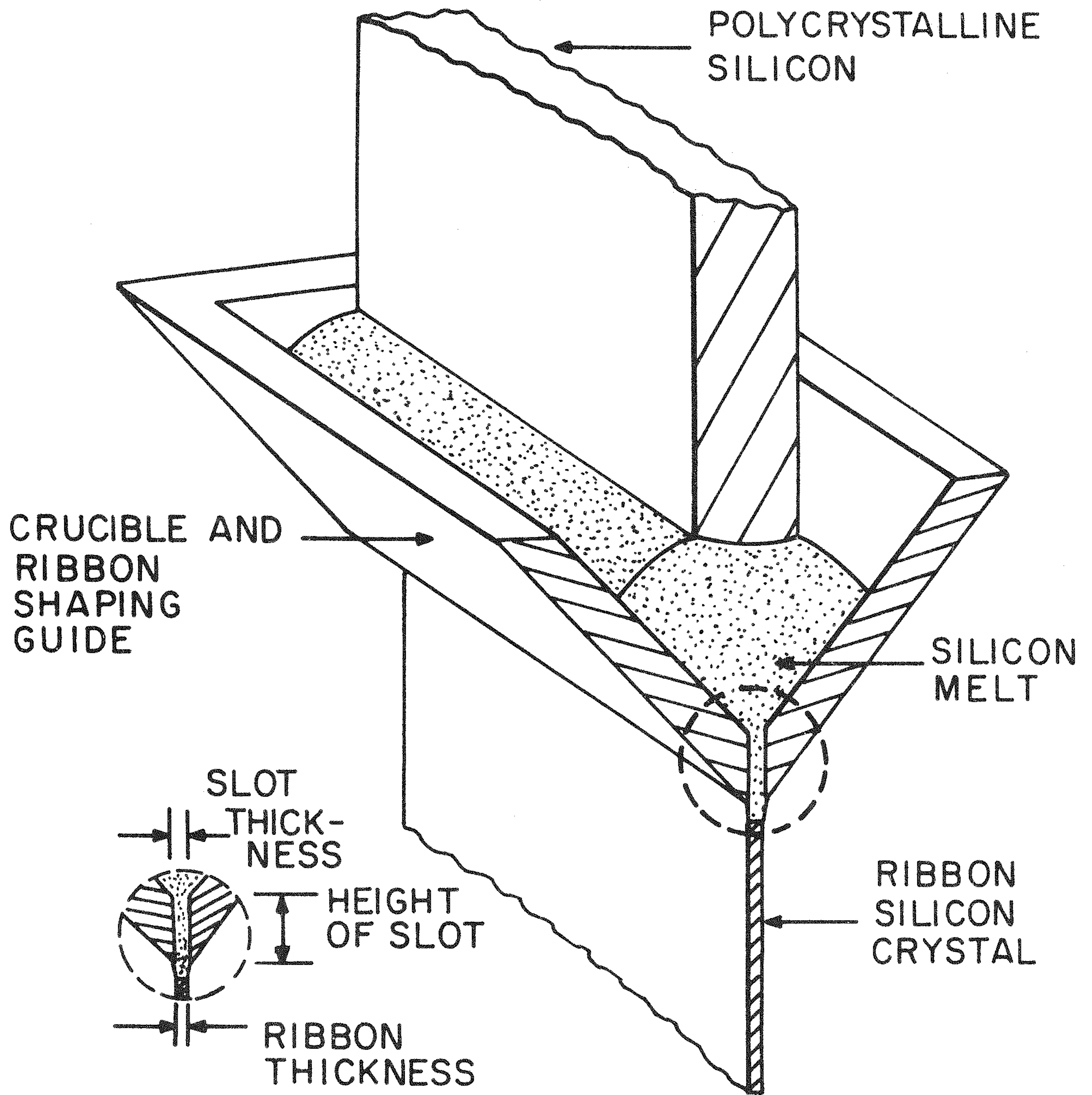

Figure 1. Schematic drawing of silicon ribbon growth by the inverted Stepanov technique (IST).

of silica at the temperatures required for the growth of silicon. This geometry has also proven to be useful in expediting the growth experiments since flat plates can be used as the liner of the die. Thus, the die slot dimensions and the position of the edge of the die in relation to the hot susceptor can be readily altered without the necessity for precision machining.

Very encouraging results had been realized in the inverted Stepanov configuration using boron nitride dies in both the flat-die and V-shaped die configurations. Stable growth of 20-mil-thick ribbons has been achieved. It was known that the boron nitride would result in heavy doping of the silicon, but the mechanical integrity at temperature and the appropriate wetting angle for Stepanov growth (110°) made it an attractive test vehicle for this process. In light of our experience with boron nitride and the experience of other investigators with silica dies [2], we had anticipated that the use of silica in the V-shaped geometry would offer an immediate solution to the boron doping problem. It was felt at that time that the major problem with silica was the softness at the growth temperature, and that the mechanical support available with the V-shaped configuration would alleviate this problem. Difficulties experienced with the growth of silica dies were initially associated with feed and/or thermal gradient problems. After a good deal of experimentation, however, it has become clear that the problems encountered have been associated mainly with the generation of silicon monoxide and the escape of the gas from the silicon-die interface. Recent effort has been directed toward the suppression of the instabilities associated with the gas evolution. This is the main topic of this progress report.

At the same time, the thermal modeling of the growth configuration has continued. The modeling has provided insight into some of the fundamental limiting factors of the growth process, and has also given guidance in the design of the apparatus.

---

2. P. C. Goundry and J. C. Boatman, "Investigation of Single Crystal Si Ribbon," AFAL-TR-66-312, Part I, Sept. 1966, and Part II, Oct. 1967.

SECTION III

PROGRESS AND TECHNICAL DISCUSSION

A. IST SILICON RIBBON GROWTH WITH SiO_2 DIE

During this reporting period, efforts were continued to solve the ribbon growth instabilities experienced when using the fused silica die in the inverted Stepanov configuration. The V-shaped susceptor/die design has been employed. Figure 2 shows the susceptor with and without pyrolytic plates. The plates are inserted to decrease the vertical temperature gradient inside the susceptor. A series of the thermal trimmers which have been tested to adjust the thermal gradient at the solid-liquid growth interface are shown in Fig. 3. The thermal trimmers consist of basically three types in various combinations. The first is a pyrolytic graphite (PG) plate with the low-conductivity "c"-axis parallel to the ribbon growth direction. The second type is a PG plate of the same orientation as the first type, which is positioned inside a rectangular graphite. The last type is an L-shaped graphite piece.

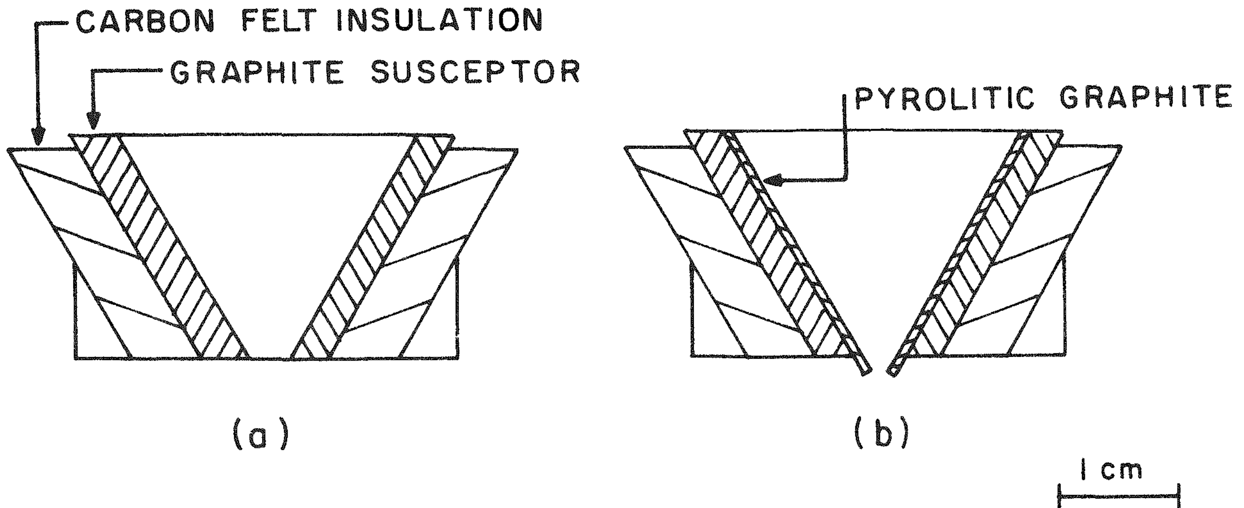

Figure 2. Cross-sectional view of the V-shaped graphite susceptor; (a) a standard type and (b) a modified susceptor to decrease the vertical temperature gradient inside the susceptor.

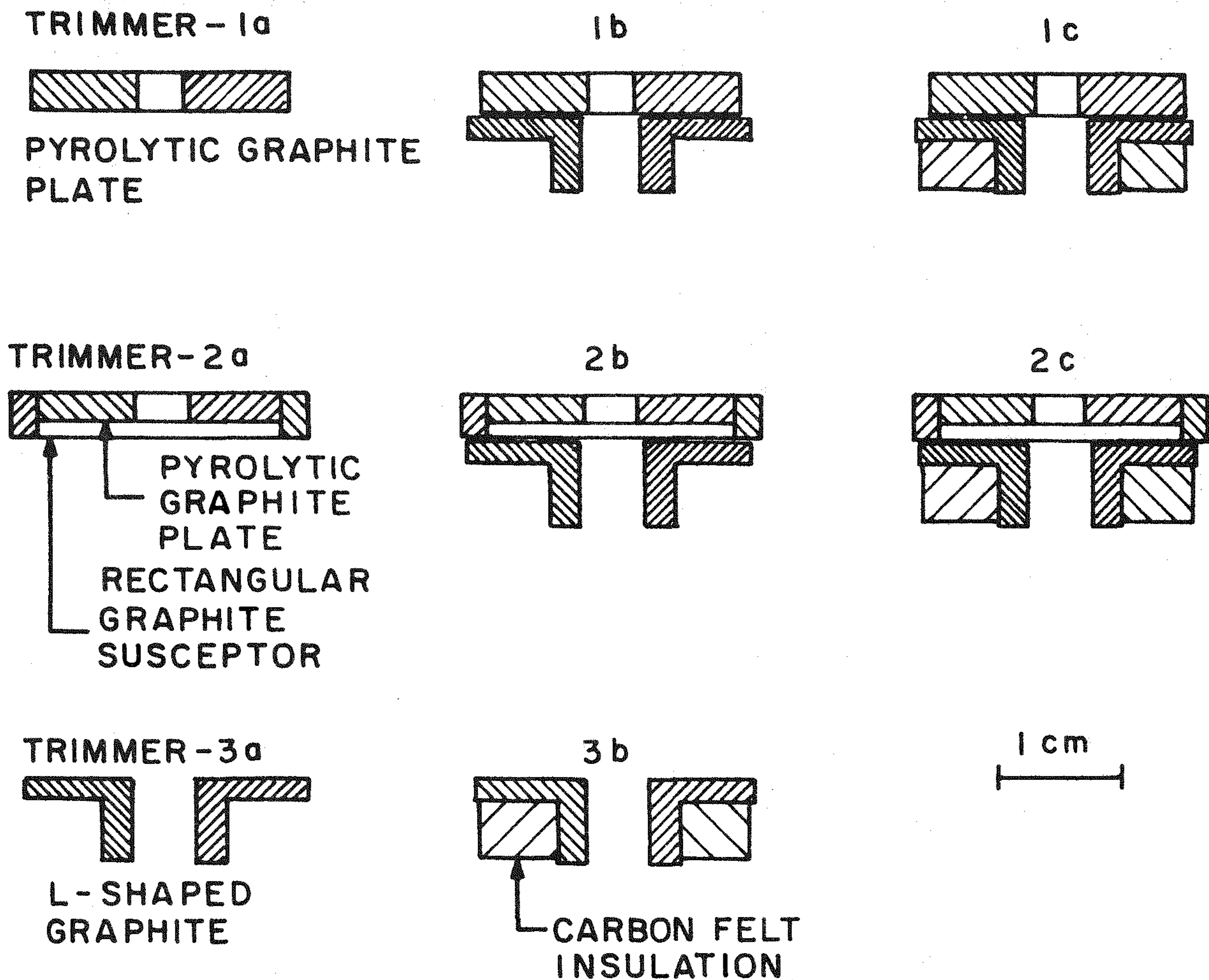

Figure 3. Cross-sectional view of the thermal trimmers used to control the thermal gradients at the solid-liquid ribbon growth interface.

Fused silica dies of three different edge shapes have been used (see Fig. 4). The size of the die slot is 0.05 x 2.5 cm wide; the height of the slot varies from 0.05 to 0.3 cm. Typically, the (110) $[\bar{1}10]$ silicon seeds are 0.04 x 1.0 to 1.5 cm wide and about 5 cm long.

The ribbon growth experiments can be divided into two categories, depending on the selection of the susceptor, thermal trimmers, and type of crucible-die being used. The first category is with the standard susceptor (Fig. 2a), flat-edged die (Fig. 4c), and various trimmers in Fig. 3. The second category is with the modified susceptor (Fig. 2b), sharp-edged die (Fig. 4a), and an L-shaped trimmer (see Fig. 3).

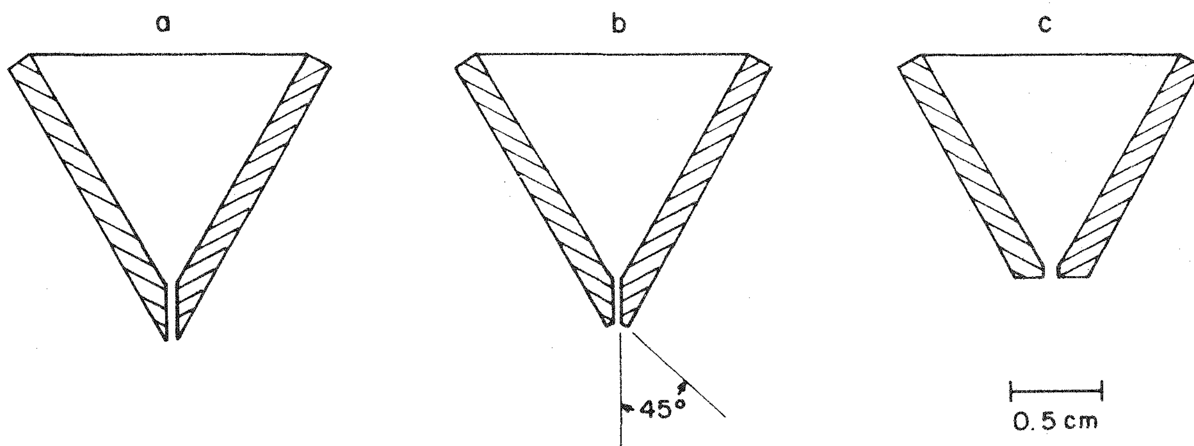

Figure 4. Cross section of fused silica dies of three different designs.

1. Ribbon Growth with the Standard V-Shaped Susceptor

The V-shaped standard susceptor and a flat-edged silica die 0.05 cm high (see Fig. 3c) were used with a series of the thermal trimmers. The horizontal and vertical temperature gradients have been measured, and ribbon growth has been tried subsequently with the same configuration as in the thermal profiling. Details of the temperature measurement have been described previously [4].

The gas flow was the same both during the profiling and the ribbon growth. Previously, a quartz pedestal with a controlled gas leak was used to generate the pressure differential, and the susceptor/die assembly was positioned on top of the pedestal [4]. This arrangement was not sufficiently versatile, however, to accommodate various types of thermal trimmers (such as L-shaped graphite). We have modified the arrangement by inverting the quartz pedestal and positioning it on top of the susceptor/die assembly.

The application of a pressure differential across the melt helped to bring the melt out of the slot and suppressed (to some extent) the mechanical vibration. The mechanical vibration is not, however, completely suppressed by the pressure differential, and the melt is continually in vertical motion both prior to seeding and during the ribbon growth after the meniscus is established outside the slot. It appears that the vibration of the melt is

caused by the formation and evolution of the silicon monoxide. This results in an oscillatory change of the contact angle.

The measured horizontal temperature distribution along the die edge and the vertical gradient below the die are given in Table 1. The horizontal temperature gradients with the pyrolytic graphite trimmers such as T-1a, T-1b and T-1c, and PG plates positioned inside a rectangular susceptor (T-2a, T-2b, and T-2c), see Fig. 3, were a few degrees per mm at the midpoint of the slot; this low gradient is within a favorable range for the ribbon growth to maintain the variation of the meniscus height within a stable range (see Thermal Analysis in Quarterly Report No. 1, p. 34 [3]).

The vertical thermal gradient was from 22 to 75°C/mm, depending on the selection of the thermal trimmer. With high vertical gradients, for instance, 57°C/mm or higher, a relatively high heat input (compared with the case with lower vertical gradients) was necessary to establish a meniscus along the seed. The ribbon growth instabilities which were already seriously limiting the ribbon growth with the lower vertical gradients became more aggravated with the increased gradient due to the increased SiO formation. The continuous increase of the ribbon thickness and freeze-over of the meniscus to the die edge during the growth were the characteristic behavior resulting from the growth instabilities observed with the SiO_2 die.

Because of the higher rf coupling of the upper section of the V-shaped susceptor, the vertical temperature gradient *inside* the susceptor led to overheating of the silica. This aggravated the growth instabilities due to the increased SiO evolution. Therefore, modified susceptors were employed (see subsection III.A.2 below).

Silica dies with flat ends have been used, and the meniscus tended to spread to the edges and resulted in freeze-over of the meniscus to the die and increase of the ribbon thickness. Similar growth instabilities were observed with silica dies with a leveled edge (see Fig. 4b).

---

3. K. M. Kim, G. W. Cullen, S. Berkman, and A. Bell, "Silicon Sheet Growth by the Inverted Stepanov Technique," Quarterly Report No. 1, ERDA/JPL/954465-76/1, prepared under Contract No. 954465 for Jet Propulsion Laboratory, June 1976.

TABLE 1. HORIZONTAL AND VERTICAL TEMPERATURE GRADIENTS MEASURED AT ABOUT 1200°C AT THE DIE EDGE AND SOME RESULTS OF THE RIBBON GROWTH RUNS USING THE STANDARD SUSCEPTOR AND A FLAT-EDGED DIE OF 0.05-cm HEIGHT.

Run No.	Horizontal Temperature (°C) at -10mm	-5mm	Midpoint	+5mm	+10mm	Vertical Temp. Gradient (°C/mm)	Thermal Trimmer in Fig. 3	Ribbon Growth Results
10-5-76 10-8-76*	1206	1204	1209	1204	1206	46	T-1b	Temp. measurement Grew ribbon 0.1 thick x 0.5 cm wide
10-4-76 10-19-76*	1210	1213	1214	1212	1208	30	T-1c	Temp. measurement Grew ribbon 0.1 thick x 0.4 cm wide
9-30-76	1210	1211	1209	1212	1213	26	T-2b	Temp. measurement
9-23-76 9-24-76*	1208	1211	1213	1208	1202	22	T-2c	Temp. measurement Meniscus size increased and melt ran out.
9-21-76 9-27-76*	1169	1163	1164	1164	1165	59	T-2a	Temp. measurement Ribbon thickness increased and froze over to die.
9-17-76	1210	1206	1202	1201	1198	65	T-2a	Temp. measurement
9-15-76	1190	1188	1184	1180	1180	75	T-1a	Temp. measurement

*Ribbon growth was carried out with the same configuration profiled above.

2. Ribbon Growth with a Modified V-Shaped Susceptor

In an effort to minimize the formation of SiO and improve "pinning" the meniscus at the die edge by decreasing the hysteresis, the V-shaped susceptor was modified to decrease the vertical gradient inside the susceptor and to avoid any unnecessary overheating of the fused silica and the liquid silicon.

Figure 5 shows the cross-sectional view of the modified susceptor in the ribbon growth configuration. The pyrolytic graphite plates (0.05 cm thick) were attached to the inner side walls of the susceptor. The high conductivity "a-b" plane of the pyrolytic graphite was parallel to the susceptor wall. Since the thermal conductivity along the "a-b" plane is about 200 times as high as along the "c"-axis, lining the susceptor with the PG plates should have decreased the vertical gradient inside the susceptor. At the same time gradients in the horizontal direction inside the susceptor should have been improved in the susceptor. The thermal gradient inside the susceptor was not measured. But with the modified susceptor the vertical gradient in the melt within the susceptor was clearly low, since during the ribbon growth the surface of the melt (melt height, 1 cm) started to freeze when the temperature at the ribbon growth interface was lowered only a few degrees below the melting point.

In order to further enhance "pinning" the meniscus at the die edge, a fused silica die with sharp edges (see Figs. 4a and 5) was employed. A pressure differential across the melt was also applied, as reported previously [4].

The horizontal temperature distribution along the die edge and the vertical gradient below the die have been measured in the same configuration as in the subsequent ribbon growth. The measured gradients are reproduced in Figs. 6(a) and 6(b). The horizontal gradient was about 3 degrees per mm at the midpoint of the slot, which is within a favorable range for the ribbon growth to restrict the variation of the meniscus height within the stable range (see "Thermal Analysis" in Quarterly Report No. 1, p. 34 [3]). The vertical gradient was 46 degrees per mm at the die edge.

---

4. K. M. Kim, G. W. Cullen, S. Berkman, and A. Bell, "Silicon Sheet Growth by the Inverted Stepanov Technique," Quarterly Report No. 2, ERDA/JPL/954465-76/2, prepared under Contract No. 954465 for Jet Propulsion Laboratory, Sept. 1976.

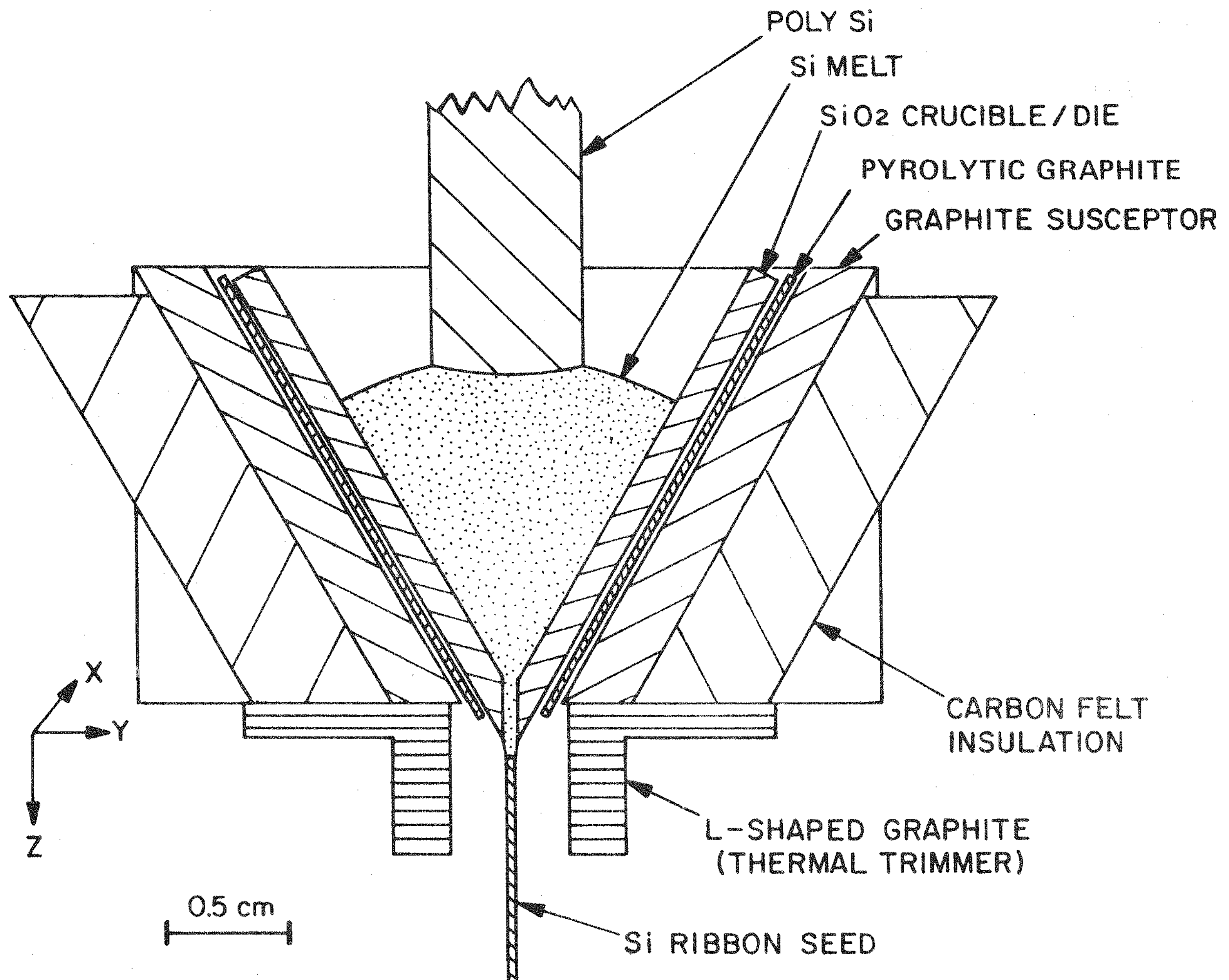

Figure 5. Ribbon growth configuration with the modified susceptor and an L-shaped trimmer.

Ribbon growth was attempted with the configuration discussed above (see Fig. 5). The pressure differential across the melt was 20 mm of oil. The size of the die slot was 0.05 x 2.5 cm wide, 0.3 cm high. A silicon ribbon seed 0.04 x 1.2 cm wide was used. Growth rates were 4 to 10 cm/h. The SiO formation was considerably less with the modified susceptor, but the hysteresis of the contact angle and the vertical vibration of the melt were still present and continued to be major causes for the growth instabilities. Only a short ribbon (4 mm long) was grown. The width decreased, while the thickness became larger than the gap of the die slot.

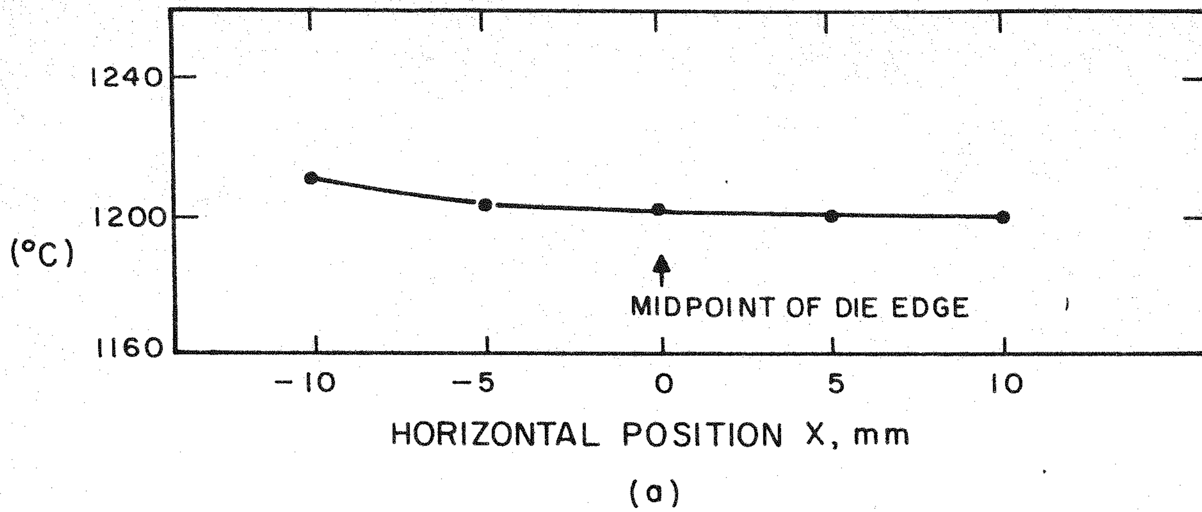

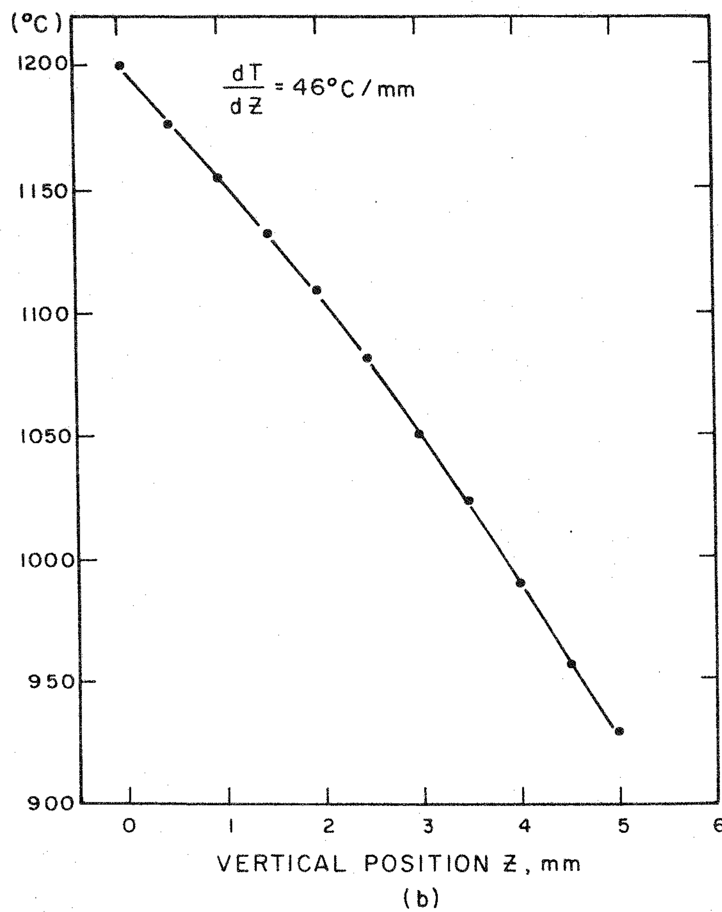

Figure 6. Thermal gradients with the modified susceptor; (a) horizontal temperature distribution along the die edge, and (b) vertical temperature gradient at the die edge.

B. SOLAR CELLS FABRICATED IN SILICON EPITAXIALLY DEPOSITED ON IST RIBBON

There has been a good deal of discussion and investigation concerning the possibility of fabricating solar cells in epitaxial layers of silicon deposited on ribbon silicon. The rationale is that not all the defects characteristic of the ribbon silicon are propagated into the epi layer. Significantly improved cell efficiencies have been realized by this process [5]. It was also recently reported [6] that a 13% efficient cell has been fabricated in epitaxial silicon deposited on heavily boron-doped ($1 \times 10^{19}/cm^3$) Czochralski silicon. In IST ribbon grown using BN dies, the boron doping has prevented direct use of the ribbon in solar cells. We have not proposed that epitaxial growth be employed with the IST ribbon, and indeed the overall objective of this program is to improve the structure of the ribbon by avoiding contamination from the die. There is a real possibility, however, that epitaxy costs can be very significantly reduced. Therefore, we thought it would be interesting to compare characteristics of cells fabricated in silicon deposited on boron-contaminated IST ribbon with the characteristics previously realized in cells fabricated in silicon deposited on EFG ribbon and in silicon deposited on heavily boron-doped Czochralski silicon.

Figure 7 shows one of the two cells fabricated on a 1.5- x 3-cm section of the same ribbon. A 50-μm p-layer (1×10^{15} cm^{-3}) was deposited and was followed by 1-μm n-layer (1×10^{18} cm^{-3}). An antireflection coating (Ta_2O_3) was applied. The I-V characteristics of the solar cells on the IST and Czochralski reference wafer are plotted in Fig. 8. The measured data of the cell parameters are reproduced in Table 2. The efficiencies of the two IST cells (AM1) were 8.1 and 8.2%, while the Czochralski cell had an efficiency of 10.2%.

---

5. H. Kressel, R. D'Aiello, P. Robinson, and S. H. McFarlane, "Epitaxial Silicon Technology For Low-Cost Solar Cells," NSF Grant AER 74-15532, Second Interim Report, Oct. 1975.

6. B. F. Williams, at Fourth Project Integration Meeting on Low-Cost Silicon Solar Array Project, ERDA/JPL, Oct. 27-28, 1976, Pasadena, Calif.

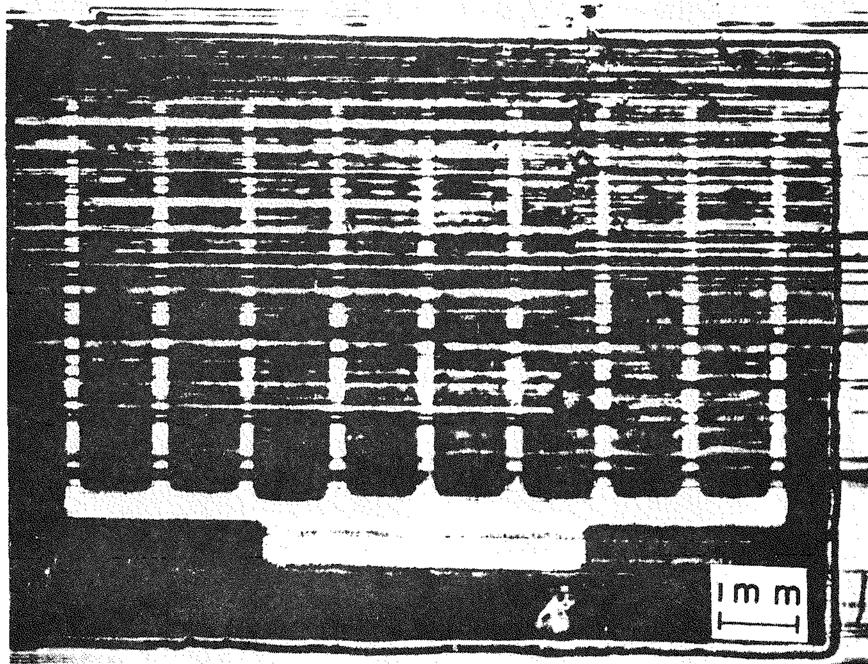

Figure 7. Photomicrograph of a solar cell fabricated in the epitaxially grown layers on the IST silicon ribbon grown with BN die.

The epitaxial cell structure was not optimized. The efficiencies can be improved by grading the doping level. It has been established that the carrier collection and cell efficiency can be increased by building in the impurity gradient in the base region to provide a drift field for enhanced carrier transport to the collecting p-n junction [5]. The efficiencies of the epitaxial solar cells on the EFG silicon ribbons with the similar structure are reported to be about 8% on the average [5]. The minority carrier lifetime was 0.3 to 0.5 μs and 0.8 μs for the IST and Czochralski based cells, respectively.

C. THERMAL ANALYSIS

During the past quarter we have used our one-dimensional computer model of growing silicon ribbon to assess the impact of the ambient thermal conditions in the growth chamber on both the maximum growth velocity and the thermal stress exerted on the ribbon during growth.

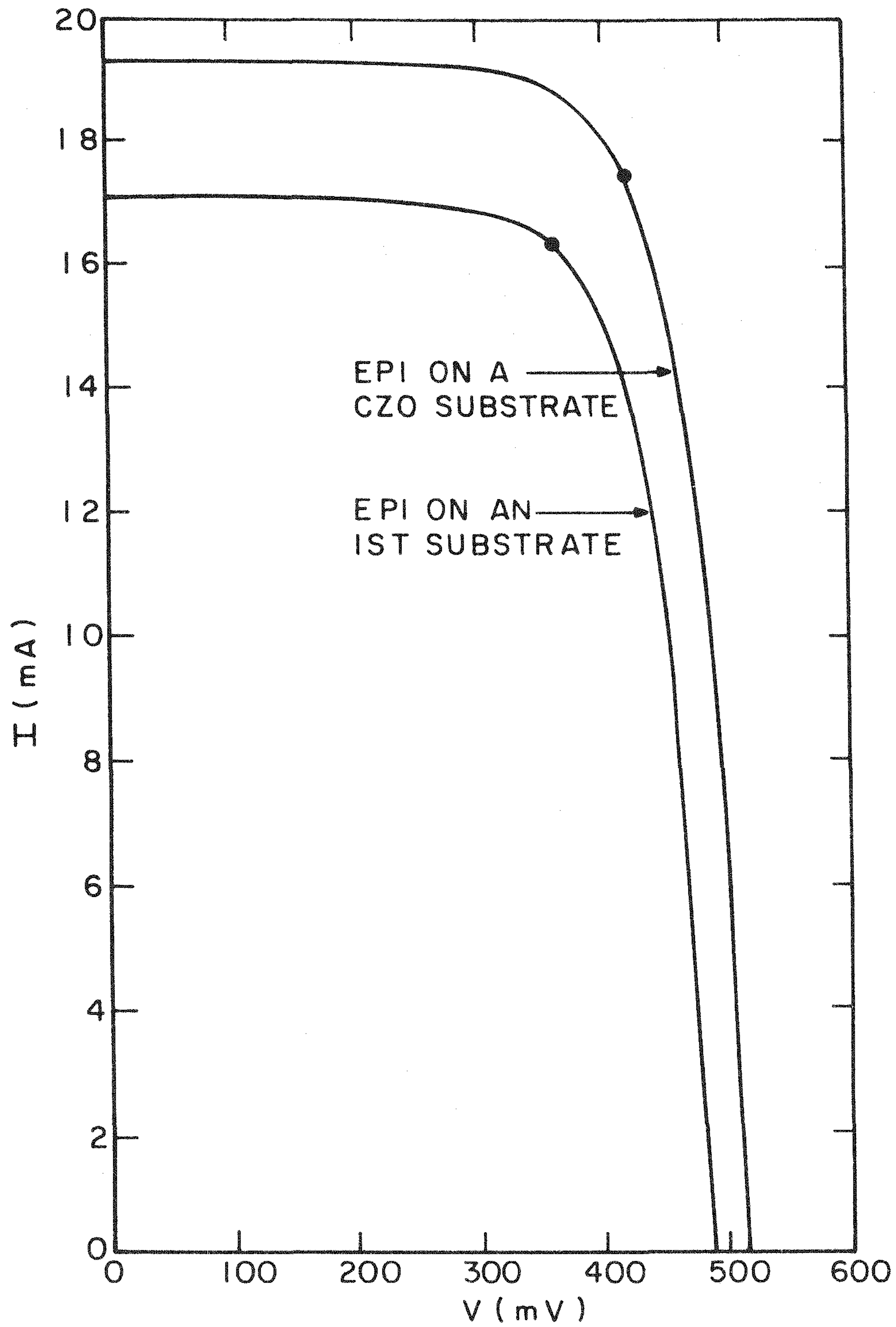

Figure 8. I-V characteristics of the epitaxial solar cells on the IST silicon ribbon and Czochralski silicon wafer.

TABLE 2. MEASURED VALUES OF THE SOLAR CELL PARAMETERS

Sample/Cell	J_{SC} (mA/cm^2)	V_{OC} (mV)	P_{MAX} (mW/cm^2)	F.F. -	η (%)
IST Cell 1	22.8	488	7.9	0.708	8.2
IST Cell 2	22.8	492	7.8	0.694	8.1
Czochralski	25.7	514	9.8	0.742	10.2

For an isotropic medium the thermal stress is clearly zero if the temperature distribution through the medium is uniform. However, it can be shown in general that even if the temperature distribution has a constant temperature gradient, $\frac{dT}{dx}$, there will be no thermal stresses. In other words, for an isotropic medium the thermal stress depends only on the curvature, $\frac{d^2T}{dx^2}$, of the temperature profile and its higher order spatial derivatives. In view of this result, in order to grow silicon ribbon with a minimum of thermal stress it is necessary to manipulate the thermal environment of the ribbon so as to produce a temperature profile in the ribbon itself which is as linear as possible. This requirement is particularly important for those regions of the ribbon where the temperature during growth exceeds the plastic temperature and even low thermal stress will cause irreversible strain, resulting in intrinsic stress at room temperature. In our analysis we have not attempted to calculate the thermal stress quantitatively, but have examined the effect of the thermal ambient of the ribbon on the curvature in the ribbon temperature profile since this will be a measure of the thermal stress.

In Fig. 9, curve I, we show the temperature profile along a 3.0-cm ribbon with a 1.0- x 0.0375-cm cross section growing with V = 0.10 cm/s. In this case the ambient temperature was uniform along the ribbon at 300°K and the ribbon clamp is also fixed at 300°K. Considerable curvature of the isotherm is evident and the magnitude of $\frac{d^2T}{dx}$ is plotted in curve I of Fig. 10 as a function of position along the ribbon. The curvature has a maximum value of 2×10^4 °K/cm^2 at the zone boundary and falls progressively in regions closer to the ribbon clamp. In Fig. 9, curve II, the profile for the same ribbon in a uniform ambient of 1300°K is shown. Since the higher ambient temperature reduces the heat loss from the ribbon to the ambient, the temperature gradient at the molten zone interface and, therefore, the maximum growth velocity are

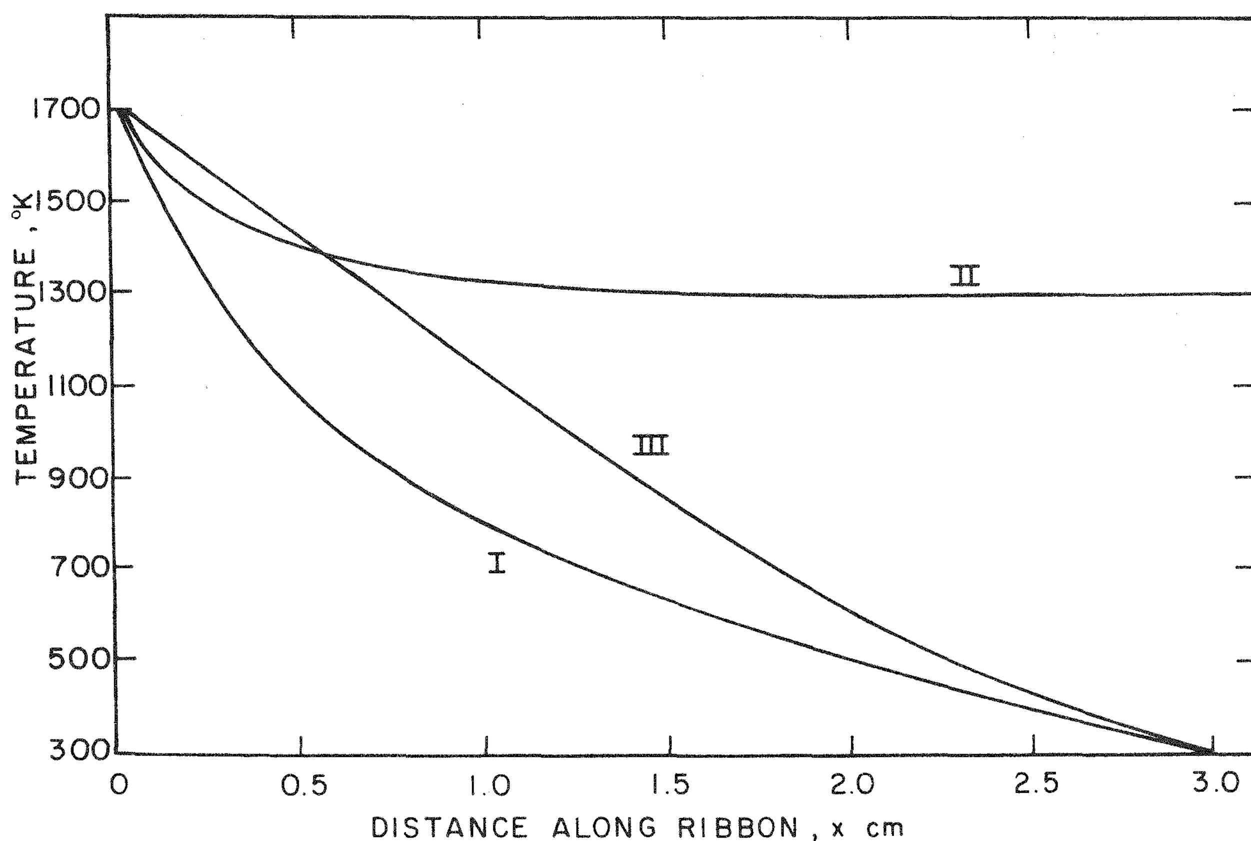

Figure 9. Ribbon temperature profiles for 0.0375 x 1.0 cm ribbon, ribbon clamp 3.0 cm from die. Curve I: 300°K uniform ambient V = 0.10 cm/s. Curve II: 1300°K uniform ambient V = 0.05 cm/s. Curve III: Linear ambient from 1650°K at the die to 300°K at the clamp, V = 0.03 cm/s.

reduced and this profile was generated when the velocity was set to 0.05 cm/s. The corresponding curvature is shown in Fig. 10, curve II and a general reduction of only about a factor of two is noted compared with the 300°K ambient case (curve I). Curve III in Fig. 9, which is significantly more linear than the others, results when the ambient temperature itself is linearly reduced from 1650°K at the die aperture to 300°K at the ribbon clamp. The magnitude of $\frac{d^2T}{dx^2}$ (curve III of Fig. 10) is reduced by about an order of magnitude from that generated in the uniform 300°K ambient case. However, the general increase in the ambient temperature now limits the rate at which heat may be dissipated

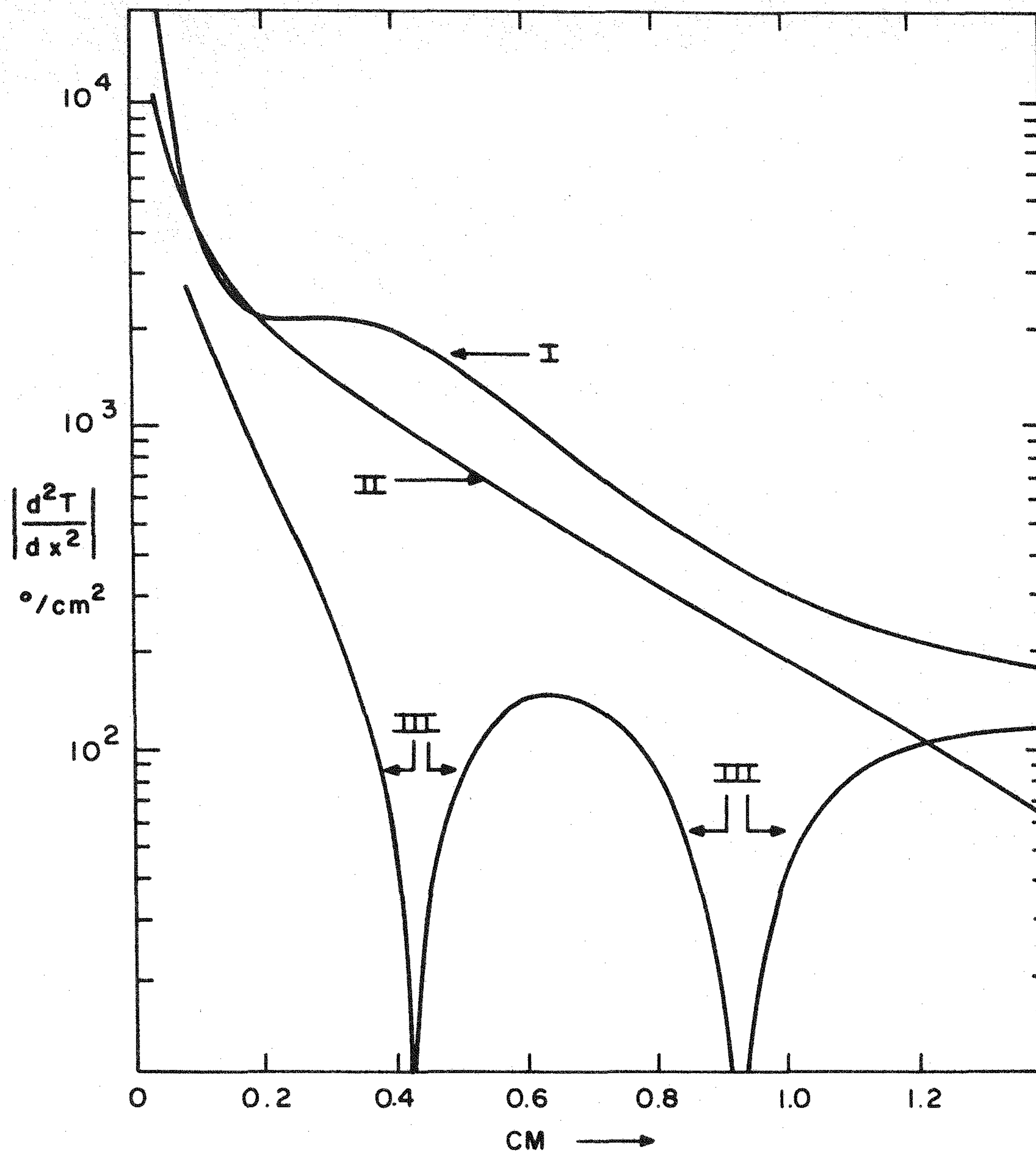

Figure 10. Curvature $\left|\frac{d^2T}{dx^2}\right|$ of the ribbon temperature profiles shown in Fig. 11.

from the ribbon surfaces to about one-quarter of that in the 300°K uniform ambient; thus, in order to linearize the temperature profile the growth rate has suffered and is limited to about 0.03 cm/s in the linear ambient temperature environment.

The thermal gradient at any point, x, along the ribbon is given by

$$\frac{dT}{dx} = \frac{Q}{KA}$$

where Q is the heat flux at that point, K is the thermal conductivity, and A is the cross-sectional area. The thermal conductivity of silicon is a function of the temperature and increases as we move from the hotter regions close to the floating zone down to the cooler regions close to the clamp. At the same time the heat flux in the ribbon reduces as we go toward the clamp due to the heat lost via radiation and convection from the ribbon surfaces to the ambient. As we have seen in Fig. 9, curve I, these two effects combine to progressively reduce the temperature gradient down the ribbon and introduce a positive curvature into the profile. Even if the ribbon were insulated to prevent heat loss to the ambient and keep Q constant all along the ribbon, curvature would still exist due to the increasingly large thermal conductivity towards the clamp. This curvature, due solely to the temperature dependence of the thermal conductivity, is shown in Fig. 11, curve I. In order to obtain a linear temperature, gradient heat must be *added* to the ribbon as we move towards the clamp in just the right quantity to compensate for the increasingly large thermal conductivity. As we have seen, heat may be added to the ribbon by arranging for the ambient temperature profile to exceed that of the ribbon itself; however, this will tend to reduce the heat conducted from the floating zone boundary, and therefore limit the growth rate. We can add heat to the ribbon from the ambient and simultaneously maintain the growth rate only by increasing the conducted heat loss to the ribbon clamp. This is achieved by reducing the separation between the die aperture and the clamp. In Fig. 11 the separation has been reduced from the 3 cm used in Fig. 9 to only 0.5 cm, and the clamp temperature is maintained at 800°K. Figure 11, curve IV shows the profile in the ribbon with a growth velocity of 0.08 cm/s when the ambient temperature varies linearly from 1600°K at the die aperture ($x = 0.0$ cm) to 1400°K at the ribbon clamp ($x = 0.5$ cm). The curvature in this case is now negative, indicating that the heat input from the ambient is overcompensating for the increasing thermal conductivity. A more linear profile results when the ambient varies linearly from 1600°K to 1300°K and this case is shown in curve III of Fig. 11 for a ribbon velocity of 0.08 cm/s. Due to the proximity of the ribbon clamp in this case the conducted heat loss to the clamp is increased to 25 W compared with only 11 W for the linear temperature ambient when the ribbon is clamped 3 cm from the die aperture.

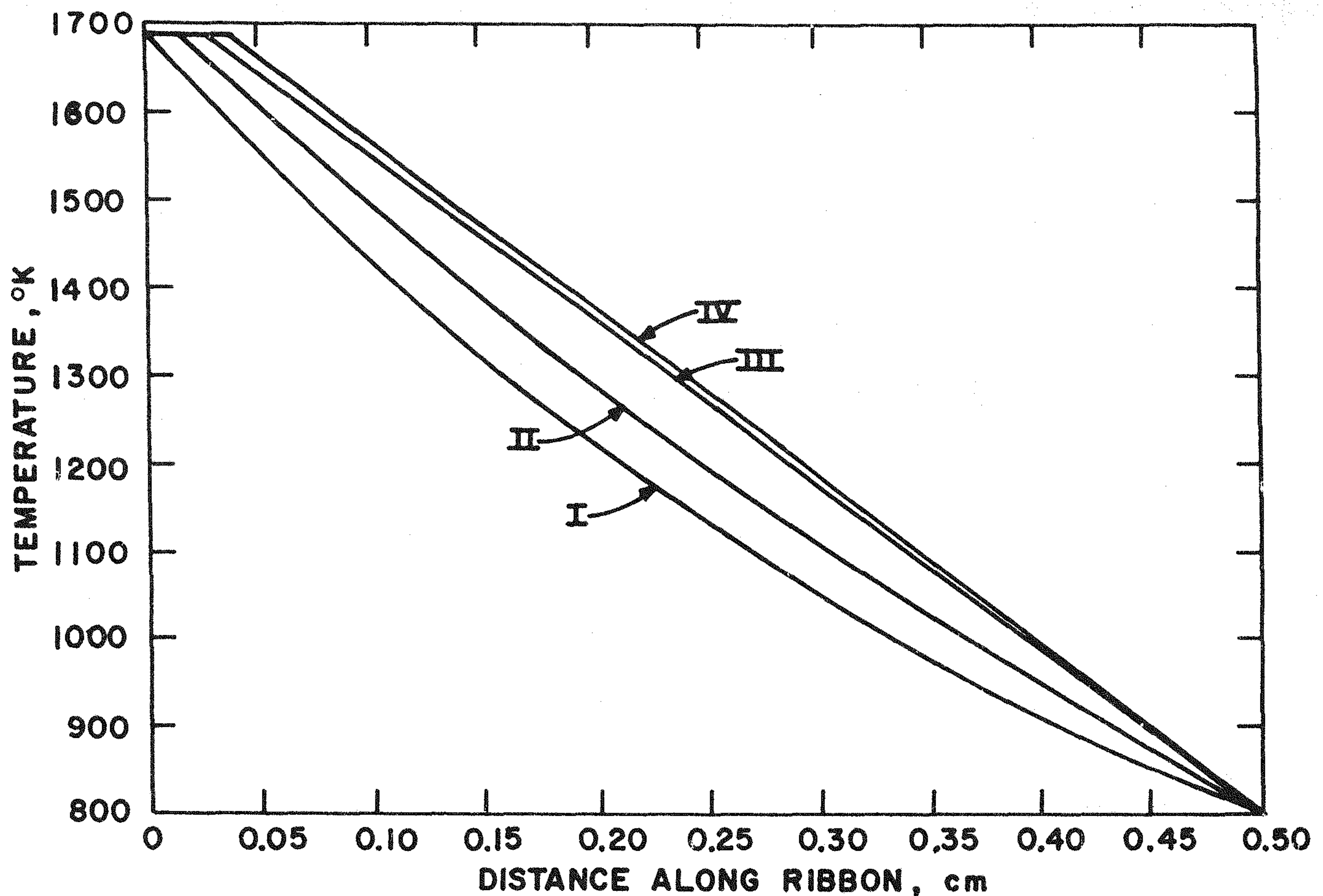

Figure 11. Temperature profile along 0.0375-cm-thick ribbon for various ambient conditions and growth rates. In all cases the ribbon is clamped at 800°K at a distance of 0.5 cm from the die aperture. Curve I: V = 0.0, no radiation or convection heat loss. Curve II: Uniform ambient 800°K, V = 0.125 cm/s. Curve III: Linear ambient 1600°K at x = 0, 1300°K at x = 0.5 cm, V = 0.08 cm/s. Curve IV: Linear ambient 1600°K at x = 0, 1400°K at x = 0.5 cm, V = 0.08 cm/s.

The resultant increase in the temperature gradient at the zone boundary permits an increase of the maximum growth velocity from 0.03 cm/s to 0.08 cm/s.

In summary, we can see that in principle it is possible to achieve a high growth rate simultaneously with a linear ribbon temperature profile by shortening the distance between the die aperture and the ribbon clamp, thereby increasing the heat flux from the molten zone boundary by increasing the conducted loss to the ribbon clamp. The radiative and convective heat transfer can then be adjusted by tailoring the ambient temperature profile to result

in a linear temperature variation along the ribbon, compensating for the temperature dependence of the thermal conductivity of the silicon.

SECTION IV
CONCLUSIONS AND FUTURE PLANS

The hysteresis of the contact angle as the result of the formation and evolution of the silicon monoxide at the interface between the silica die and the liquid silicon is a major source of the IST silicon ribbon growth instabilities. We have been trying to solve the growth instabilities with the SiO_2 die. The V-shaped susceptor has been modified to decrease the vertical gradient *inside* the susceptor in order to minimize the SiO formation and the related hysteresis. Furthermore, in an effort to improve "pinning" the meniscus at the die edge, a sharp-edged die was used. A pressure differential has been also applied across the melt to suppress the hysteresis. Various types of thermal trimmers have been tried to provide suitable thermal gradients at the solid-liquid ribbon growth interface. But so far the instabilities have not been suppressed sufficiently to allow stable ribbon growth.

Even though the fundamental feasibility of the use of the inverted Stepanov configuration has been established using the BN die, the shift from BN to SiO_2 as a die material has been more difficult than originally expected. While the difficulties associated with the formation and the evolution of silicon monoxide are not necessarily insurmountable, we feel that a more rapid progress in light of the JPL time goals will be made by using other die materials in the inverted Stepanov configuration.

REFERENCES

1. A. V. Stepanov et al., Bull. Acad. Sci. USSR, Phys. Series 33, 1826 (1969).
2. P. C. Goundry and J. C. Boatman, "Investigation of Single Crystal Si Ribbon," AFAL-TR-66-312, Part I, Sept. 1966, and Part II, Oct. 1967.
3. K. M. Kim, G. W. Cullen, S. Berkman, and A. Bell, "Silicon Sheet Growth by the Inverted Stepanov Technique," Quarterly Report No. 1, ERDA/JPL/954465-76/1, prepared under Contract No. 954465 for Jet Propulsion Laboratory, June 1976.
4. K. M. Kim, G. W. Cullen, S. Berkman, and A. Bell, "Silicon Sheet Growth by the Inverted Stepanov Technique," Quarterly Report No. 2, ERDA/JPL/954465-76/2, prepared under Contract No. 954465 for Jet Propulsion Laboratory, Sept. 1976.
5. H. Kressel, R. D'Aiello, P. Robinson, and S. H. McFarlane, "Epitaxial Silicon Technology For Low-Cost Solar Cells," NSF Grant AER 74-15532, Second Interim Report, Oct. 1975.
6. B. F. Williams, at Fourth Project Integration Meeting on Low-Cost Silicon Solar Array Project, ERDA/JPL, Oct. 27-28, 1976, Pasadena, Calif.

APPENDIX A

NEW TECHNOLOGY

There are no new technology items for this reporting period.

APPENDIX B

PROGRAM PLAN

TASKS	Apr 1976	May	Jun	Jul	Aug	Sep	Oct	Nov	Dec	Jan 1977	Feb	Mar	Apr	May	Jun
THERMAL ANALYSIS	Δ	—	—	—	—	—	—	—	—	—	—	—	—	—	Δ
• Theory (Computer Modeling)															
• Experiment															
RIBBON GROWTH	Δ	—	—	—	—	—	—	—	—	—	—	—	—	—	Δ
• Modify Model 1	Δ	—	Δ												
• Grow 15 ± 5 mil Thick 2 cm Wide Ribbon using SiO_2 Die	Δ	—	—	—	—	—	—	Δ							
• Assess 4 mil Thick Ribbon using BN Die				Δ	—	—	—	—	—	Δ					
• Develop 10 mil Thick 2 cm Wide Ribbon using SiO_2 Die				Δ	—	—	—	—	—	—	—	Δ			
• Optimize Growth for Maximum Velocity using SiO_2 Die								Δ	—	—	—	—	—	—	Δ
• Optimize Growth for Crystal Quality Considering Seeding, Die Configuration, Meniscus, SiO_2 Configuration and Other Physical Variables									Δ	—	—	—	—	—	Δ
MATERIAL CHARACTERIZATION	Δ	—	—	—	—	—	—	—	—	—	—	—	—	—	Δ
MODEL 2 DESIGN & DEVELOPMENT	Δ	—	—	—	—	—	Δ								
FINAL REPORT													Δ	—	Δ

MILESTONES*

- ↑ Complete the configuration for mechanical support of the SiO_2 die and crucible
- ↑ Preliminary design review of Model 2
- ↑ Thermal analysis (computer modeling)
- ↑ Die changes to optimize thermal gradient
- ↑ Grow 20 mil thick, 1 cm wide ribbon; growth rate 50 cm/hr
- ↑ Assess 10 mil thick ribbon with BN die; complete satisfactory seeding procedure
- ↑ Adjust thermal gradient for 2 cm wide ribbon
- ↑ Optimum s-ℓ interface/meniscus height relationship
- ↑ Thermal analysis (experimental measurement); growth rate 100 cm/hr
- ↑ Structural and electrical characterization of 15 ± 5 mil/2 cm ribbon
- ↑ Growth rate 200 cm/hr
- ↑ Structural and electrical characterization of 10 mil/2 cm wide ribbon
- ↑ Achieve 400 cm/hr growth rate and 10 mil thick 2 cm wide 30 cm long ribbon; thermal analysis completed

*These are the supplemental and/or intermediate goals to the tasks on the left.

APPENDIX C

MANHOURS AND COSTS

At the end of the second quarterly period, manhours were 2,149 and cost plus fixed fee was $73,383. Manhours for October and November were 518 and cost plus fee was $20,684. Manhours for December are estimated to be 210 and cost plus fixed fee to be $7,911. Third quarter manhours are estimated to be 728 and cost plus fixed fee to be $28,595. Cumulative manhours and cost plus fixed fee are estimated to be 2,877 and $101,978. See Figs. C-1 and C-2.

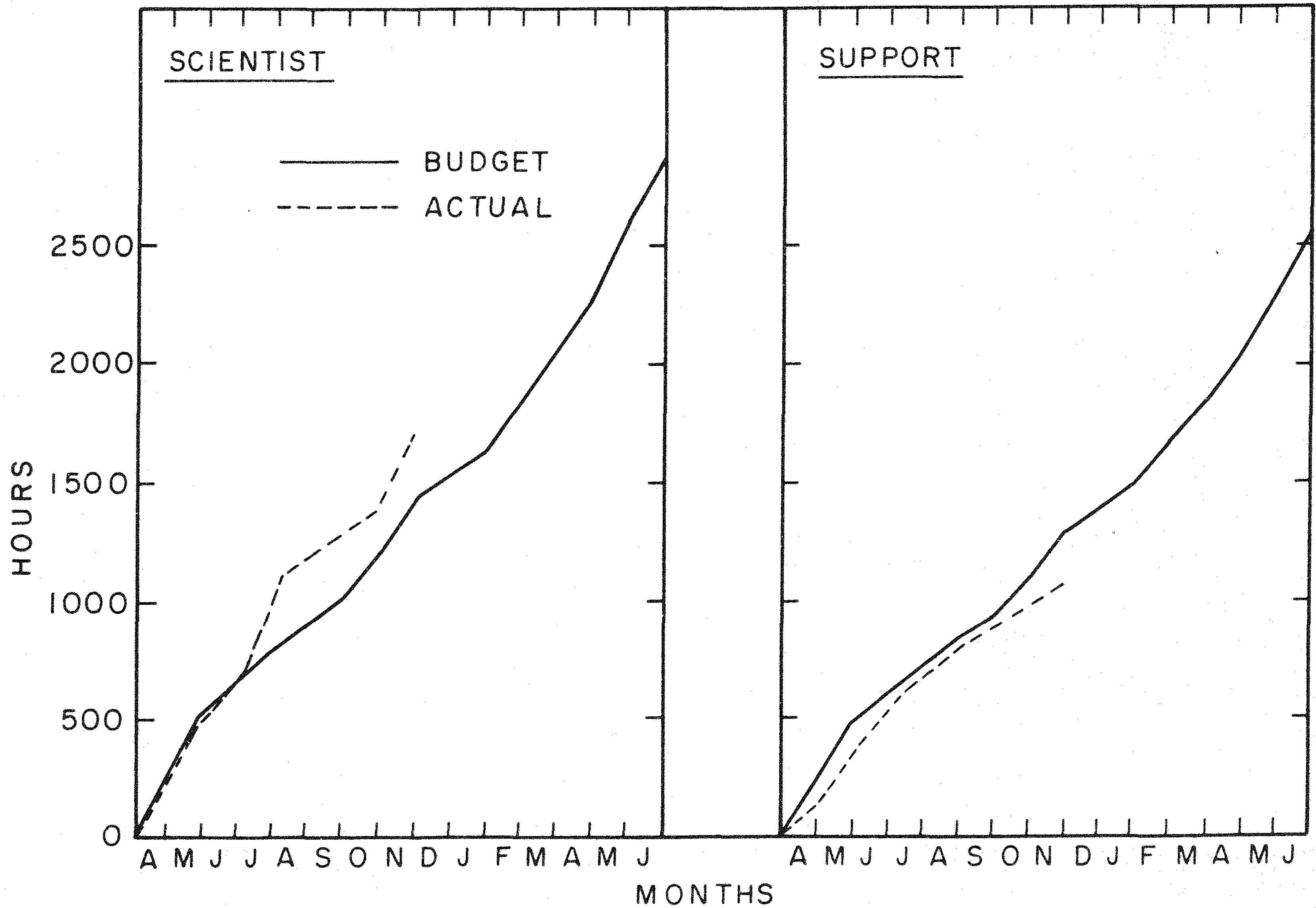

Figure C-1. Manhour chart.

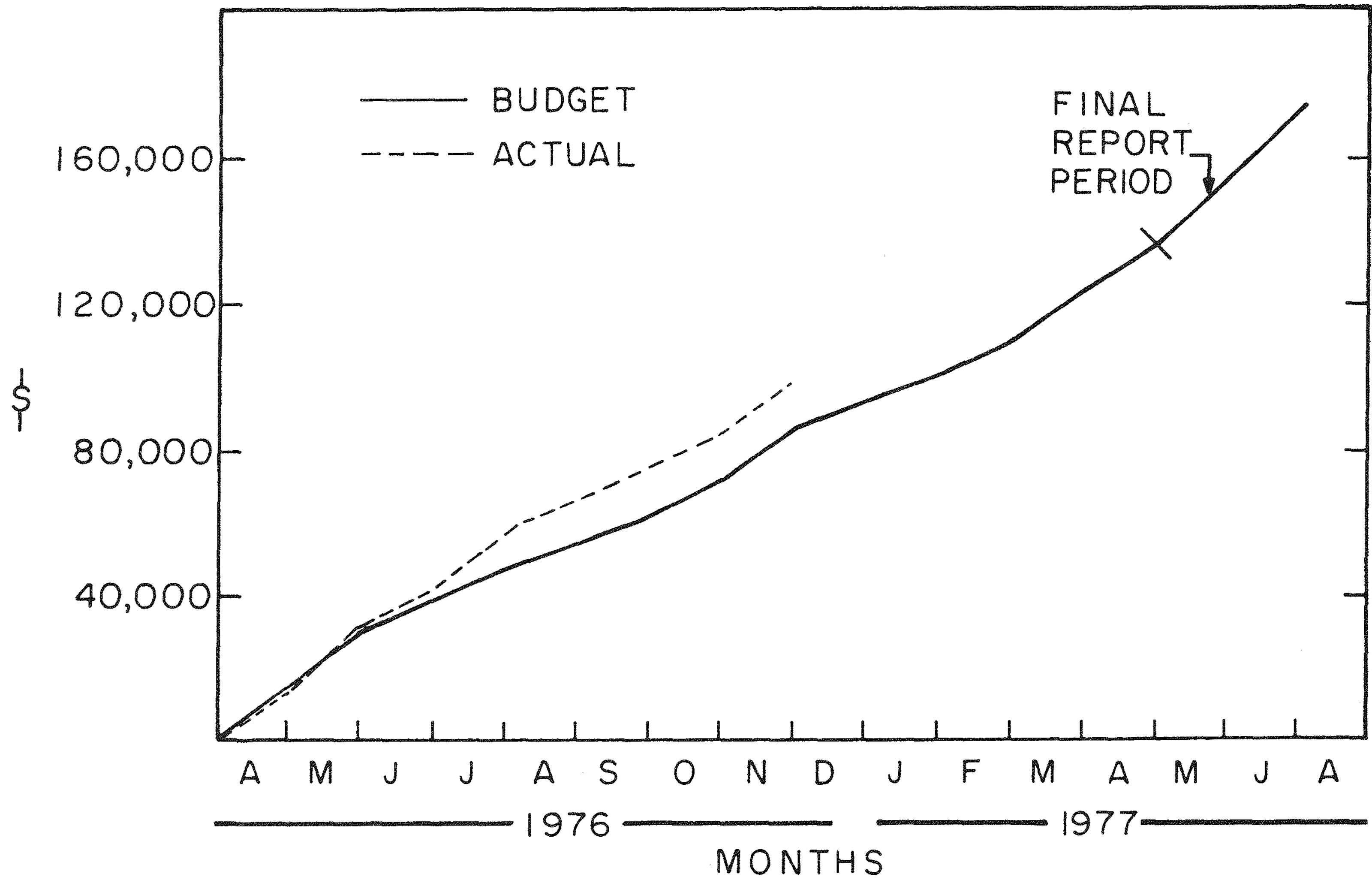

Figure C-2. Cost chart.